Journal of Hydroscience and Hydraulic Engineering
Vol. 14, No. 2, November, 1996, 9-17

THE STRUCTURE OF TURBULENT HYPERCONCENTRATED FLOWS AND THEIR RESISTANCE IN AN OPEN CHANNEL

By

H. Hashimoto

Associate Professor, Department of Civil Engineering,
Kyushu University, Fukuoka 812-81, Japan

and

M. Hirano

Professor, Department of Civil Engineering,
Kyushu University, Fukuoka 812-81, Japan

SYNOPSIS

A nondimensional parameter governing fluid-solid mixture and dry granular flows is obtained from the comparison between inertia and intergranular-stress terms in the momentum equations. Using the nondimensional parameter, a nondimensional distance from the bed is introduced for investigating velocity profiles of these flows. The flow structure of granular and inertial sublayers is found near the bed. The former sublayer has a linear velocity profile due to the major role of intergranular stresses, while the latter sublayer has a logarithmic velocity profile due to the inertial forces. Considering these sublayers in the flows, the linear and logarithmic profiles can be explained theoretically.

Surface velocity and average velocity are determined from the theoretical velocity profiles and compared with the experimental results.

INTRODUCTION

Gravity flows of hyperconcentrated mixtures of coarse sand and water have a almost linear velocity profile like a simple shear flow. The mixture flows of fine sand and water, on the other hand, have relatively uniform velocity profile similar to that of clear-water flows[1, 2]. Therefore flow resistance of the fine-sand mixtures becomes different from that of the coarse-sand mixtures. These features also can be observed in the gravity flows of dry granular materials[e.g. 3].

Arai and Takahashi [1] pointed out the importance of turbulence for the flow behavior of the fine-sand mixtures and attempted to explain the features of velocity profile. Considering the both effect of turbulence and intergranular interactions in the mixture flows, they derived an equation of velocity profile. The boundary condition for the velocity profile was determined from the velocity profile of clear-water flow. Hence the equation for mixture flow velocity includes the viscosity coefficient of clear water, although the use of the viscosity of clear water is inappropriate for the mixture flows.

Hashimoto and Hirano [4-5] proposed two nondimensional parameters for the flow situation of the hyperconcentrated sand-water mixtures. Using the parameters they examined the dependence of the flow resistance on the size of flowing materials and also discussed the structure of the flows.

The present work is an extension of the previous ones [2-5] and deals with flows with high concentration of sand, that is, the mixture and dry granular flows. For convenience such flows are termed " hyperconcentrated flows " in this paper.

We first derive a new parameter for these flows. On the basis of the discussion of the parameter, we propose a model of the flow structure near the bed. Using the model, we derive equations for estimating the velocity profiles, surface velocity and average velocity. These equations are verified with the measurements in the experiments [2, 4, 6, 7].

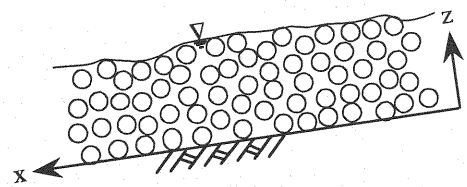

Fig. 1 Schematic diagram of a hyperconcentrated flow down a slope.

A PARAMETER GOVERNING FLOW SITUATION

For clear-water flow Reynolds number is defined as the ratio of inertial to viscous forces and is useful in the description of flow situation. Corresponding to Reynolds number there must be nondimensional parameters for the hyperconcentrated flows. Hashimoto and Hirano [4] discussed this problem by comparing inertial and intergranular forces in the momentum equation of the hyperconcentrated flows and found two parameters, which are sand concentration C and a relative flow scale L/d. Here L is a characteristic length of flows and d the diameter of sand grains. Instead of these parameters we can obtain a new parameter by referring to the discussion of Hashimoto and Hirano[4] .

The momentum equation in the x-direction for two-dimensional hyperconcentrated flows (Fig. 1) is

$$\frac{\partial u}{\partial t} + u\frac{\partial u}{\partial x} + v\frac{\partial u}{\partial z} = -\frac{1}{\rho_t}\frac{\partial p}{\partial x} + \frac{1}{\rho_t}\left(\frac{\partial \tau_{zx}}{\partial z} + \frac{\partial \tau_{xx}}{\partial x}\right) \tag{1}$$

where x = the downstream direction; z = the direction upward normal to the bed; t = time; u and v = velocity components in the x and z directions; p =pressure including the gravity component of the flows; τ_{zx}, τ_{xx}= intergranular stresses and ρ_t = the density of flows. Indicating volumetric concentration of sand by C, and densities of grain and fluid by σ and ρ, we have $\rho_t = \sigma C + \rho(1-C)$.

Many equations are proposed for the intergranular stresses in the shear flows of dry granular materials and fluid–solid mixtures [e.g.8-10]. Some of them can be written for the two-dimensional flows in the form

$$\tau_{zx} = K_{zx}\sigma d^2 F(C)\left(\frac{du}{dz}\right)^2 \tag{2}$$

and

$$\tau_{xx} = K_{xx}\sigma d^2 F(C)\left(\frac{du}{dz}\right)^2 \tag{3}$$

where K_{zx}, K_{xx} = coefficients; d = the diameter of sand grains, and F(C) = a function of C which increases with C. According to the work of Tsubaki, Hashimoto and Suetsugi [10], K_{zx} and F(C) can be written as

$$K_{zx} = \frac{\pi}{6}(0.0762+0.102\mu)\beta^2 k_M \tag{4}$$

and

$$F(C) = \frac{(C/C_*)^2}{1 - C/C_*} \tag{5}$$

where β =1.15; k_M=5; μ=0.1 and C_* = the maximum possible concentration. The equation of Tsubaki et al.[10] was originally proposed for the sand-water mixture flows. This equation is also found valid for the dry granular flows [6].

Denoting a characteristic velocity by U and a characteristic length by L, we can estimate the inertia terms as $\rho_t U^2/L$ and the intergranular-stress terms as $\sigma d^2 F(C) U^2/L^3$. The ratio of these terms is

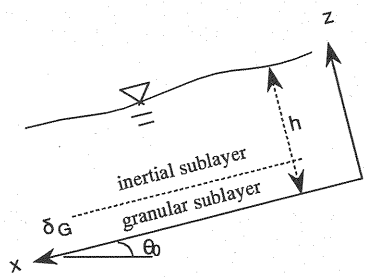

Fig. 2 The structure of a hyperconcentrated flow near the bed.

$$\frac{\text{inertia terms}}{\text{intergranular-stress terms}} = \frac{\rho_t U^2/L}{\sigma d^2 F(C) U^2/L^3} = \left(\frac{L}{d}\right)^2 \frac{\rho_t}{\sigma F(C)} \tag{6}$$

Therefore, we can see that $\frac{L}{d}\sqrt{\frac{\rho_t}{\sigma F(C)}}$ is a parameter for the hyperconcentrated flows. At smaller values of this parameter intergranular-stress terms play major role compared with the inertia terms. This represents that the effect of grain collisions becomes major. At larger values of the parameter, on the other hand, the inertia terms become important relatively to the intergranular-stress terms. This means that turbulence of the hyperconcentrated flows becomes dominant.

VELOCITY PROFILE

We discuss the velocity profiles near the bed in this chapter. Therefore we choose a distance z measured from the bottom as a characteristic length L in Eq. 6 and introduce the nondimensional distance $\frac{z}{d}\sqrt{\frac{\rho_t}{\sigma F(C)}}$ for the velocity profiles. As a result we can distinguish two layers near the bed, which can be termed granular and inertial sublayers; in the former layer the effect of grain collisions becomes major and in the latter layer the effect of the inertial forces is more important. From this discussion the flows can be modelled as shown in Fig. 2. This indicates the double structure similar to inner layer of wall turbulence, such as in clear-water flow. The almost same model was used by Egashira et al. [11] in the discussion of the effect of grain size on the velocity profile of the mixture flows. However there is no physical reason for the choice of the model. As a result there remains the thickness of granular sublayer undetermined.

We consider a steady uniform two-dimensional rapid flow at high concentration. Intergranular stresses due to grain collisions and Reynolds stresses due to the turbulent motion are important in such a flow. We use the equation of Tsubaki, Hashimoto and Suetsugi [8] for the former stresses and a mixing-length model for the latter stresses. The momentum equation in the x-direction is

$$K_{zx}\sigma d^2 F(C)\left(\frac{du}{dz}\right)^2 + \rho_t l^2\left(\frac{du}{dz}\right)^2 = \tau_0\left(1-\frac{z}{h}\right) \approx \tau_0 \tag{7}$$

where τ_0 = shear stress on the bed and concentration profile is assumed uniform for simplicity. Since we consider a region near the bed, we can neglect z/h compared with 1 on the right-hand side of Eq.7.

We first consider the granular sublayer, which is a region in the immediate vicinity of the bed. In this region the role of intergranular forces is major and that of inertial forces is minor. Therefore Eq. 7 can be written as

$$K_{zx}\sigma d^2 F(C)\left(\frac{du}{dz}\right)^2 = \tau_0 \tag{8}$$

Denoting friction velocity by u. yields $\tau_0 = \rho_t u_*^2$. Solving Eq. 8 under the boundary condition of u=0 at z=0, we obtain a linear profile of velocity. The result is

$$\frac{u}{u_*} = \frac{\xi}{\sqrt{K_{zx}}} \frac{z}{d} \sqrt{\frac{\rho_t}{\sigma F(C)}} \tag{9}$$

where ξ = a correction factor for the assumption of uniform concentration profile. Comparing values of nondimensional average velocity $\bar{u}/u_*$ calculated using Eq. 9 and according to the work of Tsubaki et al. [10], we can have the value of ξ=0.35~0.5 coresponding with C=0.25~0.5. Here $\bar{u}$ is average velocity. Since the variation of ξ is small, we use ξ = 0.4.

We second consider the inertial sublayer, which is a region on the granular sublayer. In the inertial sublayer the effect of inertial forces is major and that of intergranular forces is minor. Neglecting the first term on the left-hand side of Eq. 7, and using the relation $l = \kappa z$ for mixing length, we have

$$\rho_t(\kappa z)^2\left(\frac{du}{dz}\right)^2 = \tau_0 \tag{10}$$

where κ=the Karman constant. Denoting the thickness of granular sublayer by δ_G and velocity at $z=\delta_G$ by u_δ and solving Eq. 10, we have a logarithmic profile of velocity in the form

$$\frac{u}{u_*} = \frac{1}{\kappa} \ln\left(\frac{z}{d}\sqrt{\frac{\rho_t}{\sigma F(C)}}\right) + B \; ; \; B = \frac{u_\delta}{u_*} - \frac{1}{\kappa} \ln\left(\frac{\delta_G}{d}\sqrt{\frac{\rho_t}{\sigma F(C)}}\right) \tag{11}$$

where u_δ is given by

$$\frac{u_\delta}{u_*} = \frac{\xi}{\sqrt{K_{zx}}} \frac{\delta_G}{d} \sqrt{\frac{\rho_t}{\sigma F(C)}} \tag{12}$$

B is a function of a nondimensional thickness of granular sublayer $\frac{\delta_G}{d}\sqrt{\frac{\rho_t}{\sigma F(C)}}$. Since Eqs. 9 and 11 are a function of $\frac{z}{d}\sqrt{\frac{\rho_t}{\sigma F(C)}}$, the velocity profile can be also expresssed as

$$\frac{u}{u_*} = f\left(\frac{z}{d}\sqrt{\frac{\rho_t}{\sigma F(C)}}\right) \tag{13}$$

This relation is similar to "the law of the wall ".

THICKNESS OF GRANULAR SUBLAYER

In the calculation of velocity profiles from Eqs. 9 and 11, we must estimate a thickness of granular sublayer in advance. Therefore we determine an equation for estimating the thickness of granular sublayer in this chapter.

Fig. 3 shows the velocity profiles measured by Hirano et al. [2]. In the experiments [2] sand of different sizes was used as the bed materials. The other experimental condition was same ; the bed slope angle was 14° and the water discharge supplied per unit width at the upstream end of the flume was $q_{wo} \fallingdotseq 200 cm^2/s$. Since these experiments were made under the condition of almost same grain density and concentration, we use z/d instead of $\frac{z}{d}\sqrt{\frac{\rho_t}{\sigma F(C)}}$ as the abscissa.

We can find that the feature of velocity profiles changes at z/d=10~20. This represents the transition from the granular to inertial sublayer in the region near the bed. The elevation of the boundary between the granular and inertial sublayers can be written in the nondimensional form as

$$\frac{\delta_G}{d}\sqrt{\frac{\rho_t}{\sigma F(C)}} = 15 \tag{14}$$

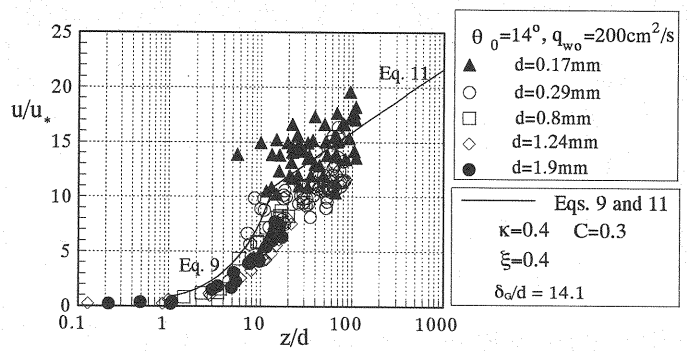

Fig. 3 Velocity profiles for the mixture flows.

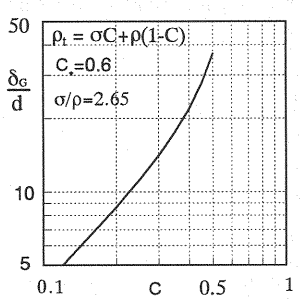

Fig. 4 The relationship between δ_G/d and grain concentration for the mixture flows.

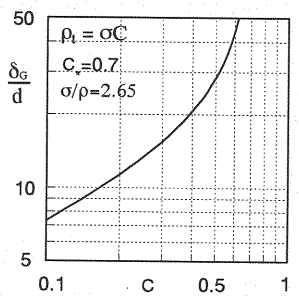

Fig. 5 The relationship between δ_G/d and grain concentration for the dry-granular flows.

The solid line in Fig. 3 shows the calculations from Eqs. 9 and 11. Here the value of κ is 0.4. We can find that these calculations are in good agreement with the measured profiles for the whole flow, although the application of Eqs. 9 and 11 is restricted to the region near the bed. The further verification of Eq. 14 is indirectly made in Figs. 6, 7, 8 and 9 in the succeeding chapter.

Figs. 4 and 5 show δ_G/d calculated from Eq. 14 for the sand-water mixtures and dry sands. In Fig. 4 the mixture density ρ_t is $\rho_t = \sigma C + \rho(1-C)$, while in Fig. 5 the mixture density ρ_t is $\rho_t = \sigma C$. It is found that δ_G/d increases with grain concentration C. This represents that the role of intergranular forces becomes major at higher concentration.

SURFACE AND AVERAGE VELOCITY

Eqs. 9 and 11 describe well the velocity profiles for the whole flow. Therefore, for covenience we extend the use of the equations to the region near the free surface for estimating surface velocity u_s and average velocity $\bar{u}$.

In the estimate of surface velocity we use Eq. 9 in the range such that $\frac{z}{d}\sqrt{\frac{\rho_t}{\sigma F(C)}} < \frac{\delta_G}{d}\sqrt{\frac{\rho_t}{\sigma F(C)}}$, while we use Eq. 11 in the range such that $\frac{z}{d}\sqrt{\frac{\rho_t}{\sigma F(C)}} > \frac{\delta_G}{d}\sqrt{\frac{\rho_t}{\sigma F(C)}}$. Further in the estimate of average velocity we integrate Eqs. 9 and 11 over depth of flow and divide them by flow depth h. For $\frac{h}{d}\sqrt{\frac{\rho_t}{\sigma F(C)}} < \frac{\delta_G}{d}\sqrt{\frac{\rho_t}{\sigma F(C)}}$ we have

$$\frac{u_s}{u_*} = \frac{\xi}{\sqrt{K_{zx}}}\frac{h}{d}\sqrt{\frac{\rho_t}{\sigma F(C)}} \qquad (15)$$

and

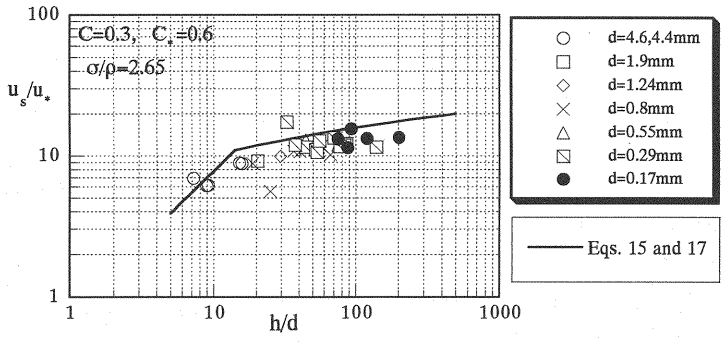

Figs.6 Relationship between nondimensional surface velocity and relative flow depth for the mixture flows.

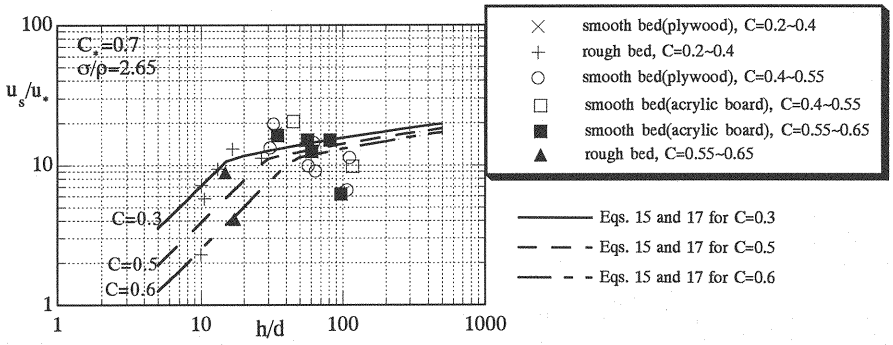

Figs.7 Relationship between nondimensional surface velocity and relative flow depth for the dry-sand flows.

$$\frac{\bar{u}}{u_*} = \frac{1}{2}\frac{\xi}{\sqrt{K_{zx}}}\frac{h}{d}\sqrt{\frac{\rho_t}{\sigma F(C)}} \tag{16}$$

Further for $\frac{h}{d}\sqrt{\frac{\rho_t}{\sigma F(C)}} > \frac{\delta_G}{d}\sqrt{\frac{\rho_t}{\sigma F(C)}}$ we have

$$\frac{u_s}{u_*} = \frac{1}{\kappa}\ln\left(\frac{h}{d}\sqrt{\frac{\rho_t}{\sigma F(C)}}\right)+B \tag{17}$$

and

$$\frac{\bar{u}}{u_*} = \frac{1}{2\sqrt{K_{zx}}}\frac{\xi}{\kappa}\frac{\delta_G}{d}\sqrt{\frac{\rho_t}{\sigma F(C)}}\frac{\delta_G}{h} + \left(\frac{u_\delta}{u_*} - \frac{1}{\kappa}\right)\left(1-\frac{\delta_G}{h}\right) - \frac{1}{\kappa}\ln\left(\frac{\delta_G}{h}\right) \tag{18}$$

Here the granular-sublayer thickness δ_G can be evaluated from Eq. 14 . From Eqs. 15, 16, 17 and 18 we can find that u_s/u_* and $\bar{u}/u_*$ are given by functions of nondimensional flow depth $\frac{h}{d}\sqrt{\frac{\rho_t}{\sigma F(C)}}$.

Fig. 6 shows the comparison between surface velocity of the mixture flows measured by Hashimoto and Hirano [7] and calculated from Eqs. 15 and 17. Here h/d is used as the abscissa

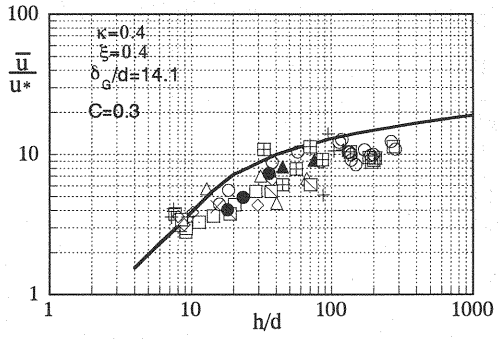

Fig. 8 Relationship between nondimensional average velocity and relative flow depth for the mixture flows.

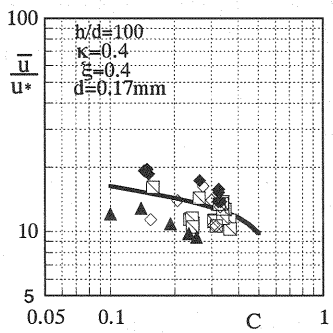

Fig. 9 Relationship between nondimensional average velocity and concentration for the mixture flows.

instead of $\frac{h}{d}\sqrt{\frac{\rho_t}{\sigma F(C)}}$, because the measurements were done under the condition of almost same grain density and concentration. The agreement between their results is excellent. Fig. 7 also shows the comparison between the measurements and calculations of surface velocity of the dry-sand flows. Here the measurements of surface velocity were done under the condition of various concentration. Three kinds of channel bed were used; one was a fixed bed roughened with same sand as flowing sand and the others were smooth fixed beds of plywood and acrylic board. The size of the roughness of plywood and acrylic board was nearly same as that of the flowing fine sand. When the flowing material is coarse and medium sand, the fixed beds were roughend with the same material. When the material is fine sand, the bed was made of plywood or acrylic board. Therefore slip velocity at the bottom was almost zero in every case of bed condition.

Fig. 8 shows the relationship between nondimensional average velocity and relative flow depth under the condition of constant concentration. Fig. 9 shows the relationship between nondimensional average velocity and concentration under the condition of almost constant relative flow depth. The theoretical and experimental results agree well.

We can conclude that the flow model shown in Fig. 2 and the nondimensional granular-sublayer thickness expresssed by Eq. 14 are appropriate for the hyperconcentrated flows.

CONCLUSIONS

The results obtained in this study are as follows:
(1) A nondimensional parameter governing flow situation are derived for hyperconcentrated flows.
(2) A distance measured vertically from the bottom is chosen as a characteristic length and the nondimensional distance is introduced for investigating the velocity profile near the bed. As a result the double structure of flow is found near the bed ; the lower structure of the effect of intergranular forces is called "granular sublayer " and the upper one of the effect of Reynolds stresses is called "inertial sublayer ".
(3) The nondimensional thickness of granular sublayer is found the value of 15. On the basis of the flow model the linear and logarithmic velocity profiles can be obtained theoretically. This corresponds to "inner layer" of wall turbulence of clear-water flow.
(4) The theoretical results of surface and average velocity agree well with their experimental ones.

REFERENCES

1. Arai M. and T. Takahashi : The mechanics of mud flows, Proc. JSCE, No.375/II-6, pp.69-77, 1986 (in Japanese).
2. Hirano M., H.Hashimoto and T.Tazaki : Experiments on the characteristics of mud flows, Proc. the 44th Annual Conference of JSCE, 2, pp.292-293, 1989 (in Japanese).
3. Hashimoto, H. : A comparison between gravity flows of dry sands and sand-water mixtures, International Workshop on Debris Flow, Kagoshima, Japan, pp.23-32, 1993.
4. Hashimoto, H. and M. Hirano : Rapid flows of sand-water mixtures at high concentration in a steep channel, Advances in Micromechanics of Granular Materials, H.H. Shen et al.(Editors), Elsevier, pp.401-410, 1992.
5. Hashimoto, H. , M. Hirano and M. S. Pallu : The structure of mud flows, Proc. the 48th Annual Conference of JSCE, 2, pp.536-537, 1993 (in Japanese).
6. Kitou, K., M. Hirano, and H. Hashimoto : Characteristics of granular flow in an inclined open channel, Proc. Hydraulic Engineering, JSCE, Vol.37, pp.617-622, 1993 (in Japanese).
7. Hashimoto, H. and M. Hirano : Gravity flow of sediment-water mixtures in a steep open channel, Journal of Hydraulic, Coastal and Environmental Engineering, JSCE No.545, pp.33-42, 1996 (in Japanese).
8. Bagnold, R.A. : Experiments on a gravity-free dispersion of large solid spheres in a Newtonian fluid under shear, Proc. Roy. Soc. A, Vol.225, pp.49-63, 1954.
9. Savage, S. B. and D. J. Jeffry : The stress tensor in a granular flow at high shear rates, Journal of Fluid Mechanics, Vol. 110, pp.255-272, 1981.
10. Tsubaki, T. , H. Hashimoto and T. Suetsugi : Interparticle stresses and characteristics of debris flow, Journal of Hydroscience and Hydraulic Engineering, Vol.1, No.2, pp.67-82, 1983.
11. Egashira, S., T. Sato and K. Chishiro : Effect of particle size on the flow structure of sand-water mixture, Annuals. Disas. Prev. Res. Inst., Kyoto Univ., No. 37 B-2, pp.359-369, 1994 (in Japanese).

APPENDIX - NOTATION

The following symbols are used in this paper:

C , C_* = volumetric concentration of sand grains in the flows and the bed;

d = diameter of sand grains;

$F(C)$ = a function of C for τ_{zx} and τ_{xx} ;

h = flow depth;

K_{zx} , K_{xx} = coefficients for τ_{zx} and τ_{xx} ;

k_M = coefficient for K_{zx} ;

l = mixing length;

L = characteristic length for flows ;

p = pressure including gravity components of flows;

q_{w0} = water discharge per unit width supplied at the upstream end of the flume;

t = time;

u, v = velocity components in the x and z directions;

u_* = friction velocity ;

u_δ = velocity at $z= \delta_G$;

u_s = surface velocity ;

$\bar{u}$ = depth-averaged velocity ;

U = characteristic velocity for flows;

x = the downstream direction;

z = the direction upward normal to the bed;

ρ, σ = densities of water and sand grains;

μ = coefficient of sliding friction between grains;

β = coefficient for K_{zx} ;

δ_G = thickness of granular sublayer;

κ = Karman constant ;

θ_0 = slope angle of flume ;

ξ = a correction factor for the assumption of uniform concentration profile ;

ρ_t = density of the mixture of sand and water;

τ_{zx} , τ_{xx} = shear stresses in the x direction on the planes perpendicular to the z and x directions; and

τ_0 = shear stresses on the bed.

(Received January 29, 1996; revised August 20, 1996)